

## Journal Pre-proofs

Proteomic and metabolomic analysis of ageing beef exudate to determine that iron metabolism enhances muscle protein and lipid oxidation

Jun Liu, Cuili Pan, Hui Yue, He Li, Dunhua Liu, Ziyang Hu, Yuanliang Hu, Xiang Yu, Weiwei Dong, Yanli Feng

PII: S2590-1575(23)00481-9  
DOI: <https://doi.org/10.1016/j.fochx.2023.101038>  
Reference: FOCHX 101038

To appear in: *Food Chemistry: X*

Received Date: 15 August 2023  
Revised Date: 12 November 2023  
Accepted Date: 25 November 2023

Please cite this article as: J. Liu, C. Pan, H. Yue, H. Li, D. Liu, Z. Hu, Y. Hu, X. Yu, W. Dong, Y. Feng, Proteomic and metabolomic analysis of ageing beef exudate to determine that iron metabolism enhances muscle protein and lipid oxidation, *Food Chemistry: X* (2023), doi: <https://doi.org/10.1016/j.fochx.2023.101038>

This is a PDF file of an article that has undergone enhancements after acceptance, such as the addition of a cover page and metadata, and formatting for readability, but it is not yet the definitive version of record. This version will undergo additional copyediting, typesetting and review before it is published in its final form, but we are providing this version to give early visibility of the article. Please note that, during the production process, errors may be discovered which could affect the content, and all legal disclaimers that apply to the journal pertain.

© 2023 The Author(s). Published by Elsevier Ltd.



## **Proteomic and metabolomic analysis of ageing beef exudate to determine that iron metabolism enhances muscle protein and lipid oxidation**

Jun Liu<sup>a,b,d</sup>, Cuili Pan<sup>c,d\*</sup>, Hui Yue<sup>a</sup>, He Li<sup>a</sup>, Dunhua Liu<sup>d\*</sup>, Ziyang Hu<sup>d</sup>, Yuanliang Hu<sup>a,b</sup>, Xiang Yu<sup>a,b</sup>, Weiwei Dong<sup>a</sup>, Yanli Feng<sup>a</sup>

<sup>a</sup> Hubei Key Laboratory of Edible Wild Plants Conservation & Utilization, College of Life Sciences, Hubei Normal University, Huangshi, 435002, China

<sup>b</sup> Hubei Engineering Research Center of Special Wild Vegetables Breeding and Comprehensive Utilization Technology, Hubei Normal University, Huangshi, 435002, China

<sup>c</sup> Key Laboratory of Animal Genetics, Breeding and Reproduction of Shaanxi Province, College of Animal Science and Technology, Northwest A&F University, Yangling, 712100, China

<sup>d</sup> Faculty of Life and Food Sciences, Ningxia University, 750021, Yinchuan, China;

\*Corresponding author: Professor Dunhua Liu and Cuili Pan

Postal address: No. 489, Mount Helan West Road, Xixia District, Yinchuan, 750000, Ningxia, China; Northwest A&F University, 22 Xinong Road, Shaanxi, 712100, Yangling, China;

E-mail address: dove\_lj@126.com and jliu@hbnu.edu.cn (Dr. Jun Liu); 13466552406@163.com (Dr. Cuili Pan); 2562948504@qq.com (Hui Yue); 3267804642@qq.com (He Li); 13350653505@163.com (Ziyang Hu); dunhualiu@126.com and ldh320@nxu.edu.cn (Professor Dunhua Liu); ylhu@hbnu.edu.cn (Professor Yuanliang Hu), yuxiang25cn@163.com (Professor Xiang Yu); 1570266392@qq.com (Dr. Weiwei Dong) fengyanli@hbnu.edu.cn (Professor Yanli Feng).

1 **Abstract**

2 The study aimed to assess differences in proteomic and metabolite profiles in ageing  
3 (1, 2, 4, and 6 days at 4°C) beef exudates and determine their relationship with beef  
4 muscle iron metabolism and oxidation. Proteomic and metabolomic analyses identified  
5 877 metabolites and 1957 proteins. The joint analysis identified 24 differential  
6 metabolites (DMs) and 56 differentially expressed proteins (DEPs) involved in 15  
7 shared pathways. Ferroptosis was identified as the only iron metabolic pathway, and 4  
8 DMs (L-glutamic acid, arachidonic acid, glutathione and gamma-glutamylcysteine)  
9 and 5 DEPs (ferritin, phospholipid hydroperoxide glutathione peroxidase, heme  
10 oxygenase 1, major prion protein, and acyl-CoA synthetase long chain family member  
11 4) were involved in iron metabolism by regulating heme and ferritin degradation, Fe<sup>2+</sup>  
12 and Fe<sup>3+</sup> conversion, arachidonic acid oxidation and inactivation of glutathione  
13 peroxidase (GPX) 4, leading to increased levels of free iron, ROS, protein and lipid  
14 oxidation ( $P < 0.05$ ). Overall, abnormal iron metabolism during ageing induced  
15 oxidative stress in muscle tissue.

16

17 **Keywords:** Exudate, Beef, Ageing, Oxidation, Iron metabolism

18

**19 1. Introduction**

20 Postmortem ageing is a common treatment in the meat industry and is a value-adding  
21 process for the muscle (Kim et al., 2018). In the process of muscle conversion into meat,  
22 there are intrinsic biophysical/biochemical changes, which subsequently have a direct  
23 impact on the quality attributes of the meat. Muscle mass is a combination of many  
24 factors, including meat taste, color, storage stability and nutrition (Yu, Li, Cheng, Brad,  
25 Kim & Sun, 2023). For example, the degradation of cytoskeletal myofibrillar protein  
26 by endogenous proteases during the ageing process has been shown to enhance the  
27 tenderization of meat. Concurrently, the liberation of flavor-related compounds,  
28 including nucleotide moieties, carbohydrates participating in the Maillard reaction,  
29 aldehydes, and ketones, as well as other lipid oxidation products, contributes to an  
30 enhancement in gustatory appeal (Kim et al., 2018; Lepper-Bllie, Berg, Buchanan &  
31 Berg, 2016). Overall, ageing had a significant positive effect on the sensory qualities  
32 of meats. Nevertheless, protracted ageing is prone to exert negative impact on the color,  
33 protein and lipid oxidative stability of meat, as well as expedite the eventual onset of  
34 meat discoloration and oxidation-driven olfactory anomalies (Yu, Cooper, Sobreira &  
35 Kim, 2021; Yu et al., 2023). Besides, the oxidation of protein can induce the forfeiture  
36 of tertiary structure and expose folded hydrophobic amino acid residues, thereby  
37 detrimentally influencing the water-binding capacity of protein (Liu, Liu, Zheng & Ma,  
38 2022). Thus, obtaining a comprehensive understanding of the early biochemical  
39 changes in postmortem is imperative in order to assess the inherent driving forces  
40 underpinning muscular quality.

41 Fresh meat is typically stored in sealed or vacuum packages, and this wet-ageing  
42 treatment is the most frequently applied ageing method (Kim et al., 2018). During the  
43 wet ageing process, substances, such as proteins and inorganic salts, dissolve in the  
44 water of the tissue medium, and are inevitably released into the package as exudate  
45 upon muscle segmentation (Setyabrata et al., 2023). Consequently, the exudate contains  
46 a plethora of biochemical components, such as lactic acid, ATP, short-chain fatty acids,  
47 amino acids, tyrosine and myoglobin, among others, that could potentially serve as  
48 substrates for analysis (Liu, Hu, Zheng, Ma & Liu, 2022). It should be noted that muscle  
49 exudate is not constant, but rather, the result of a cascade of biochemical reactions,  
50 encompassing glycogenolysis, glycolysis, oxidative phosphorylation, fatty acid  
51 metabolism, and iron metabolism, among other processes. The exudate has been  
52 reported to provide a valuable source of information, which correlates with meat quality  
53 features, including color, tenderness and water-holding capacity (Liu, Hu, Liu, Zheng  
54 & Ma, 2023; Setyabrata et al., 2023; Yu et al., 2023). It is important to emphasize that  
55 the analysis of muscle mass requires the cutting of muscle tissue, which is a destructive  
56 method (Zhang, Yu, Han, Han & Han, 2020). Exudate, on the other hand, is a non-  
57 destructive experimental sample of fluid that is released into the environment  
58 (Setyabrata et al., 2023). Overall, as an easily accessible analytical matrix, it can be  
59 used to probe the mechanisms underlying changes in muscle quality.

60 The changing patterns of muscle quality during aging have been reported, for

61 example, the effect of age on muscle metabolites, the relationship between apoptosis  
62 and tenderness and the effect of pH on meat color (Chen et al., 2020; Marcondes  
63 Krauskopf et al., 2023; Wang, Li, Zhang, Li, Yang & Wang, 2023). These studies have  
64 not addressed the mechanisms by which specific metabolic pathways occur, particularly  
65 the effect of iron on muscle metabolism and quality. This is because beef is considered  
66 red meat and contains higher levels of iron ions (Liu, Liu, Zheng & Ma, 2022). Iron  
67 metabolism is an essential intracellular metabolic process, as iron is a vital component  
68 of numerous proteins and enzymes within the biological organisms, participating in a  
69 multitude of physiological processes, such as oxygen transport, energy metabolism and  
70 immune function (Liu, Liu, Wu, Pan, Wang & Ma, 2022). On the other hand,  
71 disturbances in iron metabolism may result in the overproduction of free radical  
72 substances, provoking oxidative stress within cells (Wang et al., 2023). Nevertheless,  
73 the iron metabolism process is a sophisticated biological system, and it is necessary to  
74 use effective techniques to elucidate the variation in muscle quality throughout the  
75 ageing process by exploring the metabolic pathways. Utilizing metabolomics analysis  
76 of exudate, we have identified reductions in muscle quality resulting from anomalies in  
77 iron metabolism during the ageing process (Hu et al., 2022; Liu et al., 2023).  
78 Proteomics and metabolomics techniques have achieved ubiquitous application in the  
79 quest for biological markers of meat quality traits, concurrently allowing for the  
80 characterization of the interplay between a multitude of biological functions, including  
81 protein and metabolite chemistry, signal transduction pathways and gene expression  
82 patterns (Huang et al., 2023). Thus, these techniques provide a comprehensive account  
83 of the mechanisms responsible for alterations in the components and biological  
84 processes relevant to meat quality.

85 Considering the intricate nature of iron metabolism and meat quality change  
86 characteristics, the exudate samples from bovine muscles aged 1, 2, 4 and 6 days were  
87 collected, and examined through proteomics and metabolomics analyses, revealing a  
88 comprehensive picture of the proteins and metabolites present in the exudate mixtures.  
89 A combination of proteomics with bioinformatics was used to analyze muscle iron  
90 metabolism pathways during ageing and explore the intrinsic mechanisms affecting  
91 muscle quality. This study evaluates the potential application of exudate for probing the  
92 substrates of muscle quality changes and provides new insights into the patterns of  
93 muscle quality changes during aging. The study may provide fundamental data for meat  
94 quality analysis, prediction and development of characterization marker systems.

## 95 **2. Materials and Methods**

### 96 *2.1 Sample collection*

97 The muscle samples were aged and exudates (EXU) were collected according to our  
98 previous report (Liu et al., 2023). In brief, eight adult Qinchuan cattle (bulls, 18-24  
99 months of age, weighing approximately 400 kg) were slaughtered at a commercial  
100 slaughterhouse (Yitai Co., Yongning, China) according to Chinese livestock slaughter  
101 protocols. Muscle samples (*M. longissimus lumborum* muscles) were collected after  
102 slaughter, and were divided into cubes with sides of 2.5 cm thickness and  $100.0 \pm 2.5$

103 g weight, placed on PET plastic trays and wrapped in polyvinyl chloride cling film. The  
104 muscle samples were divided into 4 groups of 6 pieces each and aged at 4°C for 6 days  
105 (Foshan City Aslok Refrigeration Equipment Co., Ltd., Foshan, China). EXU were  
106 aspirated on days 1, 2, 4 and 6, named as EXU1, EXU2, EXU4 and EXU6, respectively.  
107 Samples were taken at the center of the muscle tissue for freezing in liquid nitrogen and  
108 then stored in a -80°C cryopreservation chamber (Qingdao Haier Biomedical Co.,  
109 Qingdao, China) for proteomic, metabolomic, physiological and biochemical analyses.

## 110 *2.2 Determination of iron ion content in exudate and beef*

111 The collected exudate samples were thawed at 2-4°C and centrifuged at  $3000 \times g$ , 4°C  
112 for 15 min. The supernatant was removed and the iron content in EXU was determined  
113 using a fully automated biochemical analyzer (Chemray 240, Radu Life, Shenzhen,  
114 China) according to the instructions of the iron assay kit (Huili Biotechnology Co., Ltd.,  
115 Changchun, China).

116 The 30 g of muscle were minced, and  $10.00 \pm 0.02$  g of minced meat were added into  
117 100 mL of deionized water, then homogenized for 60 s and centrifuged at  $12,000 \times g$   
118 for 10 min. The supernatant was separated through an Amicon Ultra-15 ultrafiltration  
119 centrifuge filter (3,000 MW cut-off) (Millipore, Massachusetts, USA), centrifuged at  
120  $4,500 \times g$  for 50 min, and the liquid was collected at the bottom of the centrifuge tube.  
121 Then 4 mL of the filtrate was pipetted, and the free iron content was measured by ICP-  
122 OES (Agilent, Santa Clara, CA, USA).

## 123 *2.3 Antioxidant status of exudate and beef*

124 The EXU was thawed in an ice-water bath, centrifuged at  $3500 \times g$ , 4°C for 10 min,  
125 and the supernatant was used for antioxidant analysis. The absorbance values were  
126 measured at 450 nm and 412 nm (UV-9000S Metash Instruments co, Ltd, Shanghai,  
127 China) to calculate the total superoxide dismutase (T-SOD) and glutathione peroxidase  
128 (GSH-PX) activities, respectively, referring to the kit manufacturer's instructions  
129 (Jiancheng BI, Nanjing, China). Carbonyl, sulfhydryl and malondialdehyde (MDA)  
130 levels were determined according to Liu et al. (2022) utilizing the manufacturer's  
131 instructions of a commercial kit (Jiancheng BI, Nanjing, China).

## 132 *2.4 Muscle tissue reactive oxygen species (ROS) levels*

133 ROS levels in muscle tissue were measured by the 2,7-dichlorofluorescein diacetate  
134 (DCFH-DA) method according to Zhang, Yu, Han, Han & Han (2020). Briefly,  $5.00 \pm$   
135  $0.05$  g of pulverized muscle samples were mixed with 20 mL of prechilled potassium  
136 phosphate buffer (10 mM Tris, 10 mM sucrose, 0.8% NaCl, 0.1 mM EDTA-2Na, pH  
137 7.4), and then homogenized for 60 s and centrifuged at  $10,000 \times g$ , 4°C for 20 min.  
138 Then, 5 mL supernatant was mixed with 5 mL potassium phosphate buffer (containing  
139  $10 \mu\text{M}$  DCFH-DA) and incubated at 37°C in the dark for 35 min. A fluorescence  
140 spectrophotometer (Yidian Scientific Instruments Co., Shanghai, China) with an  
141 excitation wavelength of 480 nm and an emission wavelength of 525 nm was used to

142 measure fluorescence intensity before and after incubation. The ROS level was  
143 expressed as the ratio of fluorescence intensity before and after incubation to protein  
144 concentration and incubation time.

### 145 *2.5 Proteomics analysis*

146 The EXU samples were thawed in an ice water bath after removal from the -80°C  
147 refrigerator. Exudates were thawed only once to avoid repeated freeze-thawing. Then  
148 100 µL of exudate were added to 400 µL of SDT lysate buffer (4% sodium dodecyl  
149 sulfate, 100 mM Dithiothreitol, 150 mM Tris-HCl, pH 8.0) and the mixture was  
150 sonicated in an ice bath for 2 min. Undissolved impurities were removed using  
151 centrifugation at 16,000 × g for 15 min, and the supernatant was collected, and the  
152 concentration of exudate proteins was quantified according to the instructions of the  
153 BCA Protein Assay Kit (Bio-Rad, CA, USA).

154 Protein digestion, TMT peptide labelling, peptide classification and LC-MS/MS  
155 analysis were performed referring to our previous report (Liu et al., 2022). In a nutshell,  
156 protein extracts from muscle samples were subjected to trypsin (Promega Co.) digestion  
157 and purified peptides were collected. The extracted peptides were labelled using TMT  
158 labelling kits according to the manufacturer's instructions (Thermo Fisher, MA, USA),  
159 and the dried peptides were fractionated using a high pH reversed-phase column  
160 (Pierce™ High pH Reversed-Phase Peptide Fractionation Kit, Thermo Fisher, MA,  
161 USA). The solubilized peptides were chromatographed (LC-MS) using a nanolitre flow  
162 rate chromatography system (Thermo Fisher, MA, USA). The peptides were separated  
163 and analyzed by DDA (data dependent acquisition) mass spectrometry using a mass  
164 spectrometer (Thermo Fisher, MA, USA).

165 The resulting LC-MS/MS raw RAW files were imported into the search engine  
166 Sequest HT in Proteome Discoverer software (version 2.4, Thermo Scientific) for  
167 database searching. The database used for the library search was uniprot-Bos taurus  
168 (Bovine) [9913]-47135-20220613.fasta from the URL  
169 <https://www.uniprot.org/taxonomy/9913> protein database with protein entry: 47135;  
170 download date. 2022.06.13. The main library search parameters were set as shown  
171 below.

### 172 *2.6 Metabolomics analysis*

173 The untargeted metabolomic analysis of the exudate was performed according to our  
174 previous report (Liu et al., 2022). Untargeted metabolomics profiling was analyzed with  
175 a UPLC-ESI-Q-Orbitrap-MS system (Ultra High Performance Liquid Chromatography,  
176 Nexera X2 LC-30AD, Shimadzu CO., Kyoto, Japan; Q Exactive Plus combined  
177 quadrupole Orbitrap mass spectrometer, Thermo Scientific, CA, USA). Samples  
178 consisted of muscle exudate aged for 1, 2, 4 and 6 days and four sets of quality control  
179 (QC) samples with an equal volume mix of exudate. Metabolites were extracted from  
180 the exudate residue by vortexing 100 µL of a sample with 400 µL of 4°C methanol-  
181 acetonitrile (v/v, 1:1) and sonicated in an ice bath for 1 h. The mixture was incubated at

182 -20°C for 1 h and then centrifuged at  $14,000 \times g$ , 4°C for 20 min. The supernatant was  
183 collected and freeze-dried under a vacuum. The metabolites were separated using  
184 hydrophilic interaction liquid chromatography (HILIC) after re-dissolution using 50%  
185 acetonitrile and filtration through 0.22  $\mu\text{m}$  cellulose acetate. Mass spectrometric  
186 detection was performed using electrospray ionization (ESI) in positive and negative  
187 modes to acquire metabolite MS data.

## 188 2.7 Statistical analysis

189 *P*-values for proteins and metabolites were calculated using one-way analysis of  
190 variance (ANOVA) for multiple analyses with R 4.0.1 (). Metabolites with variable  
191 influence on projection (VIP) values  $>1.0$  and *P*-value  $<0.05$  were considered to be  
192 statistically significant. Proteins with fold change (FC)  $\geq 1.2$  or  $\leq 0.83$  and *P*  $<0.05$  were  
193 considered to be statistically significant proteins. The main components of the  
194 combined metabolomics and proteomics analysis project flow using R 4.0.1 and  
195 Cytoscape 3.8.2 include network analysis, metabolite and protease correspondence  
196 table, combined metabolism-protein analysis KEGG metabolic pathway enrichment,  
197 and Total KEGG pathway analysis. All physicochemical experiments were performed  
198 in three parallel experiments. Data were tallied in Microsoft Excel using one-way  
199 analysis of variance (ANOVA) in SPSS 25 (IBM, NY, USA), followed by Tukey's  
200 analysis to calculate statistical differences between samples, with *P*-values  $< 0.05$   
201 considered statistically different.

## 202 3. Results

### 203 3.1 Exudate and beef oxidation status

204 As shown in **Fig. 1**, the iron ion levels in EXU did not differ significantly from 1 to 4  
205 d and increased significantly (*P*  $< 0.05$ ) at 6 d with a growth rate of 148.37% compared  
206 to 1 d. Free iron levels in beef tissues significantly increased (*P*  $< 0.05$ ) from 1 to 6 d.  
207 The increase in iron ion levels was accompanied by a significant decrease in T-SOD  
208 and GSH-PX activity in the exudate (*P*  $< 0.05$ ). In contrast, beef tissue ROS levels  
209 increased significantly (*P*  $< 0.05$ ) from 1 to 6 d, with a growth rate of 176.38%  
210 compared to 1 d. Using carbonyl and sulfhydryl groups and malondialdehyde (MDA)  
211 to characterize the protein and lipid oxidation status of exudate and beef, exudate and  
212 beef exhibited the same status, with increased protein carbonyl and MDA levels and  
213 decreased sulfhydryl levels at 1-6 d, indicating enhanced protein and lipid oxidation.  
214 Notably, the increase in total protein levels in the exudate indicates the presence of  
215 macromolecules available for proteomics analysis.

### 216 3.2 Metabolomics profiling

217 Using a non-targeted metabolomics assay, 572 and 305 metabolites were identified  
218 from beef exudate in positive and negative ion mode (POS and NEG), respectively. To  
219 obtain a comprehensive overview of metabolite profiles and trends to assess whether  
220 metabolites could be used for differential metabolites (DMs) screening and  
221 bioinformatics analysis, principal component (PCA) and partial least squares (PLS-DA)



222 analyses were performed in the identified metabolites. As shown in **Fig. 2** a and d, PCA  
223 analysis showed no separation of quality control samples (QC) in POS and NEG,  
224 indicating reliable results for metabolite detection based on the LC-MS/MS system.  
225 PCA analysis showed a better overall separation compared to EXU1, but with some  
226 overlap. As shown in **Fig. 2** b and e, pairwise comparison of the PLS-DA model for  
227 EXU1 and EXU2&4&6 metabolites revealed a good degree of separation between  
228 EXU1 and EXU2&4&6, indicating that the models reasonable and the identified  
229 metabolites can be used for the next step of analysis.

230 As shown in **Fig. 2** c and f, a total of 278 DMs were identified in the POS and  
231 NEG using *t*-test ( $P$ -value  $\leq 0.05$ ) and variable influence on projection (VIP)  $\geq 1$  as  
232 screening criteria (**Table S1**). Cluster analysis of the identified DMs was performed  
233 (**Fig. 2g**), where the color change in the same column showed the pattern of metabolite  
234 variation (upregulation-orange, downregulation-blue). In addition, the DM  
235 superclasses were classified using KEGG, and the DMs were mainly organic acids and  
236 derivatives (39), organoheterocyclic compounds (32), lipids and lipid-like molecules  
237 (21), phenylpropanoids and polyketides (15), nucleosides, nucleotides and analogues  
238 (14), benzenoids (13), and organic oxygen compounds (12).

### 239 3.3 Proteomics profiling

240 The protein composition of the four groups of exudate samples was examined by TMT  
241 proteomics. **Fig. 3a** shows the expression patterns of the proteins in different groups  
242 with correlation coefficients (Corr)  $> 0.995$ , indicating the reliable results based on the  
243 LC-MS system. A total of 1957 proteins were identified by annotation of protein  
244 peptides. The differentially expressed proteins (DEPs) were screened with a fold  
245 changes (FC) of  $>1.2$  fold (up  $> 1.2$ , down  $< 0.86$ ) and a *t*-test  $P$ -value  $< 0.05$  as the  
246 criteria (**Fig. 3** b-d). A total of 295 DEPs were identified (**Table S2**). The clustering  
247 heat map analysis of DEPs is shown in **Fig. 3e**. The similar color of the same group of  
248 proteins indicates that the corresponding proteins have the same expression pattern,  
249 showing good intra-group similarity and inter-group variability. Secondly, the  
250 clustering heat map showed the changes of protein expression, with orange color  
251 indicating up-regulated protein expression and blue color indicating down-regulated  
252 protein expression (**Fig. 3e**). Overall, the proteomic identification of proteins in exudate  
253 showed reliable results, and relevant DEPs were identified for subsequent  
254 bioinformatics analysis.

### 255 3.4 Analysis of the KEGG enrichment pathway

256 **Fig. 4** a and b show the KEGG pathways that DMs and DEPs are enriched to, involving  
257 mainly cellular processes, environmental information processing, human diseases,  
258 metabolism and organismal systems. Among them, the pathways involved in DMs are  
259 mainly ferroptosis, ABC transporters, purine metabolism, carbon metabolism,  
260 biosynthesis of amino acids, and protein digestion and absorption. The pathways  
261 involved in DEPs are mainly endocytosis, protein processing in endoplasmic reticulum,  
262 oxidative phosphorylation and thermogenesis. Since iron metabolism may affect

263 cellular processes, the top 10 cellular processes in the pathway, as shown in **Fig. 4c**,  
264 including tight junction, regulation of actin cytoskeleton, focal adhesion, autophagy -  
265 animal, cellular senescence, phagosome, ferroptosis, peroxisome and adherens junction  
266 were further screened in the study.

267 The metabolic pathways involved in DMs and DEPs were screened using  
268 metabolomics and proteomics approaches (**Fig. 4 a and b**), and a combined analysis of  
269 metabolomics and proteomics was performed using the KEGG pathway as a vector.  
270 Interworking Network and Venn diagram showed the status of KEGG pathway  
271 interactions involving metabolomics and proteomics (**Fig. 4 d and e**), with 58 metabolic  
272 pathways screened by metabolomics and proteomics identified 49 metabolic pathways,  
273 of which 15 metabolic pathways overlapped between the two. **Fig. 4e** shows the 15  
274 metabolic pathways shared by metabolomics and proteomics, and notably, the iron  
275 metabolic pathway (ferroptosis) was found among the pathways.

### 276 *3.5 Iron metabolic pathway analysis*

277 To better understand the linkages between DMs, DEPs and metabolic pathways  
278 involved in iron metabolism, DMs and DEPs involved in iron metabolism (ferroptosis)  
279 were identified. As shown in **Fig. 5 a and b**, four DMs were identified, including L-  
280 glutamic acid, arachidonic acid, glutathione and gamma-glutamylcysteine. Five DEPs  
281 were found, including ferritin, phospholipid hydroperoxide glutathione peroxidase,  
282 heme oxygenase 1, major prion protein and acyl-CoA synthetase long chain family  
283 member 4. The pathway-pathway interaction network diagram drawn by four DMs and  
284 five DEPs (**Fig. 5c**) showed that the process of iron metabolism (ferroptosis) was not  
285 isolated, and the process of iron metabolism was jointly regulated by the interaction  
286 between DMs and DEPs.

## 287 **4. Discussion**

288 Ageing is the most common treatment of meat in order to achieve satisfactory meat  
289 quality (della Malva, Gagaoua, Santillo, De Palo, Sevi & Albenzio, 2022). However,  
290 not all effects of the ageing process are positive, and longer ageing times lead to reduced  
291 oxidative stability, which in turn reduces the quality of the meat (Yu et al., 2023). After  
292 slaughter, muscle oxidation is inevitable and involves a series of metabolic pathways,  
293 including glycolysis, mitochondrial respiratory chain and nitric oxide accumulation  
294 (Chen et al., 2022; Liu, Hu, Zheng, Ma & Liu, 2022). Iron ions in muscle oxidation are  
295 usually overlooked. However, our previous study found that iron overload induced  
296 protein and lipid oxidation (Liu, Liu, Zheng & Ma, 2022). Currently, the analysis of  
297 meat quality and potential biochemical processes during ageing relies on muscle tissue  
298 (della Malva et al., 2022). Muscle tissue has similar metabolite types and levels to its  
299 exudates, which reflects the potential value of exudates for providing information about  
300 meat characteristics (Castejón, García-Segura, Escudero, Herrera & Cambero (2015).  
301 In this research, 877 metabolites and 1957 proteins were identified in exudate, and the  
302 physicochemical characteristics of exudate, including iron content, protein and lipid  
303 oxidation status, were consistent with beef expression trends (**Fig. 1**), indicating that

304 exudate can be used for characterizing the underlying biochemical processes of beef  
305 oxidation.

306 In the case of beef, a red meat is because bovine muscle is a  $\beta$ -red fiber and  
307 contains high amounts of iron, which is present in the muscle in the form of heme. Iron-  
308 containing hemoglobin is retained in muscle tissue in the form of blood residues. In  
309 addition, iron is present in macromolecular fractions, such as cytochromes, iron-sulfur  
310 proteins and iron carrier proteins (Liu et al., 2022). These iron-containing proteins  
311 provide carriers for the release of free iron or low-molecular-weight iron, the released  
312 iron ions generate hydroxyl radicals ( $\bullet\text{OH}$ ) through the Fenton reaction, and  $\bullet\text{OH}$  is  
313 considered the most powerful oxidant known to oxidize lipids and proteins, leading to  
314 the deterioration of meat quality (Zhang et al., 2022). Ferroptosis has been found in  
315 muscle tissues, and the accumulation of free iron is central to the generation of ROS  
316 and mediates cell death. Thus, it is clarified that iron ions act as a destabilizing factor  
317 that reduces muscle quality through metabolic activity (Liu, Hu, Ma, Yang, Zheng &  
318 Liu, 2023). Notably, we previously used exudate to investigate the mechanisms of beef  
319 quality change, and found that abnormal iron metabolism activated the ferroptosis  
320 pathway, inducing oxidative stress in muscle tissue cells (Liu et al., 2022). Ferroptosis  
321 is a non-apoptotic regulation of cell death by iron-dependent lipid peroxidation due to  
322 unstable iron accumulation and glutathione peroxidase (GPX) 4 inactivation. At the  
323 core of this is the induction of lipid reactive oxygen species (ROS) accumulation by  
324 iron overload through the Fenton reaction (Xia et al., 2021). Free iron levels in exudate  
325 and beef significantly increased during ageing (**Fig. 1a**,  $P < 0.05$ ), leading to an increase  
326 in iron metabolic instability. At the same time, muscle ROS levels were accompanied  
327 by the accumulation of iron ions, leading to the oxidation of proteins and lipids (**Fig.**  
328 **1i**). Overall, further studies in the expression patterns of metabolites and proteins in  
329 exudate are needed to reveal the mechanisms of iron metabolism in muscle oxidation  
330 during aging.

331 Homeostatic imbalances in iron metabolism affect normal physiological pathways,  
332 and iron overload is a critical factor in iron metabolism (Xie, Fang & Zhang, 2023).  
333 Bioinformatic analysis of exudate metabolites and proteins identified the only iron  
334 metabolic process, namely ferroptosis (**Fig. 4f**). As illustrated in **Fig. S1**, ferroptosis  
335 involves inactivation of GPX4 antioxidant action, lipid peroxidation, degradation of  
336 iron-containing proteins and conversion of iron ion valence states. As the name implies,  
337 iron accumulation is the key hub of ferroptosis, and the ferroptosis pathway shows the  
338 degradation of ferritin and heme to release free iron ions (**Fig. S1**). Ferritin is an iron  
339 storage protein that plays a central role in regulating iron metabolism and maintaining  
340 iron homeostasis. Ferritin is normally present in cells as ferritin light chain (FTL),  
341 heavy chain 1 (FTH1) and the constituent complexes, which can store more than 2000-  
342 4500  $\text{Fe}^{3+}$  under normal physiological conditions. Consequently, ferritin can efficiently  
343 regulate intracellular iron homeostasis (Zhang, Yu, Song, Xiao, Xie & Xu, 2022).  
344 Notably, FTH1 and FTL exhibit different functional activities for iron binding. FTH1  
345 has oxidase activity and converts soluble free iron in the cytoplasm into ferritin  
346 precursors that enter the ferritin structural domain and then bind to the inner ferritin

347 space after conversion by the action of FTL (Zhang et al., 2022). Liu, Hu, Ma, Wang  
348 & Liu (2023) examined ferritin levels during beef refrigeration, and found that FTL and  
349 FTH1 exhibited different degradation states, which verified the different activity  
350 between FTH1 and FTL. The level of ferritin in the exudate tended to decrease during  
351 ageing (**Fig. 5b**), consistent with the findings of Liu et al. (2023). During ageing  
352 intracellular homeostasis is imbalanced and the selective autophagy receptor nuclear  
353 receptor coactivator (NCOA) 4 is activated to ensure cell survival, during which the  
354 inevitable NCOA4 binds to FTH1 and transports ferritin to the autophagosome for  
355 degradation (ferritinophagy), with eventual release of free iron (Xia et al., 2021). **Fig.**  
356 **S1** shows the iron accumulation pathway of heme degradation by heme oxygenase (HO)  
357 1. Heme is a ferroporphyrin compound composed of divalent iron with four porphyrin  
358 rings, primarily myoglobin and hemoglobin (Liu et al., 2022). The level of heme in  
359 muscle is related to the type of animal and the part of the meat. Lombardi-Boccia,  
360 Martinez-Dominguez, & Aguzzi (2002) examined the heme iron contents in different  
361 animals and different parts, and found that beef heme iron content was significantly  
362 higher than other meats. Thus, heme-rich beef has a higher potential for iron ion release.  
363 Heme degradation relies mainly on the HO-1 catalytic system to release free iron  
364 (Singhabahu, Kodagoda Gamage & Gopalan, 2023). Free iron more readily mediates  
365 protein and lipid oxidation and is not heme (Zhang et al., 2022). Proteomics results  
366 showed a significant upregulation of HO-1 expression (**Fig. 5b**). Liu, Hu, Ma, Yang,  
367 Zheng & Liu (2023) analyzed the protein levels of HO-1 and heme, and found that the  
368 two were negatively correlated, consistent with the proteomics results. Overall, the  
369 degradation pathway of ferritin and heme during ageing is a key mechanism to induce  
370 iron sagging.

371 Iron ions can affect iron metabolism through transmembrane transport, with iron  
372 ions transferred intracellularly mainly via the transferrin (TF) and metal cation  
373 symporter ZIP8 (MCSZ8) pathways (**Fig. S1**). Proteomics identified a major prion  
374 protein (D5G2D5) that facilitates the conversion of trivalent to divalent iron ions (**Fig.**  
375 **5b**), and its protein level decreased with increasing ageing duration. Iron ions are more  
376 sensitive to iron metabolic processes due to their higher oxidative activity as a result of  
377 valence conversion (Xia et al., 2021). However, the reduced level of soft virus protein  
378 inhibited the cross-transport of iron ions by MCSZ8, while reducing the oxidative  
379 activity of divalent iron ions. On the other hand, the TF pathway is considered to be the  
380 main cell membrane ferric ion transport system (Wang, Wei, Ma, Qu & Liu, 2022),  
381 while there are different protein levels between TF and MCSZ8. Unfortunately, the  
382 effect of ferric ion transport across the membrane on cellular iron metabolism remains  
383 unknown.

384 Another hallmark event of iron metabolism disorders leading to ferroptosis is lipid  
385 oxidation, where polyunsaturated fatty acids (PUFAs) of cell or organelle membranes  
386 are susceptible to oxidation by ROS generated through the Fenton reaction and generate  
387 lipid peroxides (LPOs), the aggregation of which leads to membrane instability or even  
388 rupture, resulting in cellular homeostatic imbalance or even cell death (Liang, Zhang,  
389 Yang & Dong, 2019). Acyl-Co A synthetase long chain family (ACSL) 4 is a

390 modulator of lipid metabolism. ACSL4 converts PUFAs to membrane phospholipids-  
391 phosphatidylethanolamine (PE) due to its thioesterified activity, forming PUFA-CoA.  
392 PUFA-CoA is a precursor of PUFA-phospholipids (PUFA-PLs), and PUFA-PLs are  
393 further oxidized by lipoxygenase to produce lipid peroxides (LOOHs, ·OH, etc.).  
394 Interestingly, arachidonic acid (AA) and epinephrine acyl contain a PE fraction, which  
395 facilitates lipid oxidation even more (Kagan et al., 2017; Yang, Kim, Gaschler, Patel,  
396 Shchepinov & Stockwell, 2016). The levels of both AA and ACSL4 increased during  
397 ageing (**Fig. 5a** and **b**), and the increase in AA content provides more substrate for  
398 ACSL4, which inevitably increases lipid peroxidation. There was a significant increase  
399 in lipid peroxidation (MDA level) in exudate and beef during late ageing (**Fig. 1g**,  $P <$   
400  $0.05$ ). It is noteworthy that ROS generated by the Fenton reaction are not specific for  
401 the oxidation of macromolecules and attack macromolecular components, such as  
402 proteins and DNA while oxidizing lipids, which inevitably enhances the oxidative state  
403 of the muscle (Liu et al., 2022). The increased carbonyl and sulfhydryl levels in exudate  
404 and beef indicate increased protein oxidation during ageing (**Fig. 1 e** and **f**,  $P <$   $0.05$ ).  
405 Lipid and protein oxidation are not independent processes, but rather promote each  
406 other. For example, lipid peroxides bind to muscle proteins, and LOOHs and ·OH  
407 promote protein oxidation more rapidly (Liu et al., 2022).

408 The level of ROS generated by disorders of iron metabolism depends on  
409 sophisticated homeostatic regulatory functions of cells, and the classical mechanism of  
410 scavenging is through the glutathione peroxidase (GPX) 4 antioxidant system (Wang  
411 et al., 2022). GPX4 belongs to the glutathione peroxidase family, which specifically  
412 scavenges a wide range of lipid peroxides from cell membranes, and GPX4 is  
413 dependent on glutathione (GSH) as a reducing agent in its peroxidase action. GSH is a  
414 tripeptide synthesized from cysteine, glutamate and glycine. Cystine-glutamate  
415 antiporter pumps glutamate out of the cell and pumps cystine into the cell in a 1:1 ratio.  
416 The cystine delivered to the cell is reduced to cysteine by  $\beta$ -mercaptoethanol, which is  
417 used to synthesize the antioxidant GSH (Bi et al., 2023; Wang et al., 2022; Yang et al.,  
418 2016). GPX4 and GSH levels decreased during ageing (**Fig. 5 a** and **b**), indicating  
419 GPX4 may have a diminished effect on lipid peroxide scavenging, which can lead to  
420 an enhanced cellular or muscle oxidative state. In contrast, L-glutamic acid and gamma-  
421 glutamylcysteine levels were upregulated during aging, where higher levels of L-  
422 glutamic acid inhibited cystine transport, leading to a decrease in the content of GSH  
423 precursors (Liu et al., 2023). Carbon metabolism, 2-oxocarboxylic acid metabolism and  
424 biosynthesis of amino acids were also found to affect L-glutamic acid levels through  
425 glutamate-enriched metabolic pathways (**Fig. 5c**). For example, the 2-oxoglutarate  
426 dehydrogenase complex during carbon metabolism converts glutamate by catalyzing  
427 the conversion of 2-oxoglutarate generated in the tricarboxylic acid cycle (TCA)  
428 pathway, which may also lead to elevated glutamate levels (Weidinger et al., 2023). It  
429 is speculated that elevated gamma-glutamylcysteine levels may be associated with  
430 reduced glutathione synthetase activity, which requires further validation. The  
431 regulation of GSH-GPX4, an important intracellular antioxidant does not proceed  
432 independently, interacting with metabolic pathways, such as carbohydrates and amino  
433 acids, was not effective in avoiding oxidative stress induced by iron metabolism,

434 reducing the quality of meat during aging. In general, the ferroptosis process is  
435 dependent on the accumulation of free iron, inactivation of antioxidant systems, and  
436 cell membrane lipid oxidation. These processes not only promote cell death, but also  
437 lead to deterioration of muscle quality through accumulation of ROS and lipid  
438 peroxides.

## 439 **5. Conclusions**

440 Exudate and beef were found to have similar patterns of change in terms of iron ions  
441 and oxidation. A combination of proteomics and metabolomics was used to identify the  
442 metabolite and protein changes that can be used to characterize the underlying  
443 biochemical pathways in muscle tissue. Overall, beef exudates provide valuable  
444 information to understand metabolic mechanisms during muscle aging. A total of 15  
445 shared KEGG pathways were identified, and iron metabolism was mainly manifested  
446 as ferroptosis. The 4 DMs and 5 DEPs involved in the ferroptosis pathway may induce  
447 oxidative stress and even cell death through the regulation of free iron accumulation,  
448 cell or organelle membrane oxidation and GPX4, exacerbating muscle protein and lipid  
449 oxidation during aging.

## 450 **Appendix A. Supplementary material**

451 Supplementary Fig. S1.

452 Supplementary Table S1.

453 Supplementary Table S2.

## 454 **Funding**

455 This study was financially supported by the Ningxia Natural Science Foundation  
456 (2022AAC02021), Hubei Normal University 2023 introduced talent research start-up  
457 fund, and Excellent Young and Middle-Aged Science and Technology Innovation Team  
458 Plan Project of University in Hubei Province (T2022028).

## 459 **Data Availability Statement**

460 Not applicable.

## 461 **Acknowledgments**

462 Thanks to Gaolong Yin at Shanghai Bioprofile Technology Company Ltd. for his  
463 technical support in proteomics. Thanks to Prof. Deming Gong of the New Zealand  
464 Institute of Natural Medicine Research for proofreading the language of the article.

## 465 **References**

466 Bi, Y., Liu, S., Qin, X., Abudureyimu, M., Wang, L., Zou, R., Ajoalabady, A., Zhang, W., Peng,  
467 H., Ren, J., & Zhang, Y. (2023). FUNDC1 interacts with GPx4 to govern hepatic ferroptosis

- 468 and fibrotic injury through a mitophagy-dependent manner. *Journal of Advanced Research*.  
469 <https://doi.org/10.1016/j.jare.2023.02.012>
- 470 Castejón, D., García-Segura, J. M., Escudero, R., Herrera, A., & Cambero, M. I. (2015).  
471 Metabolomics of meat exudate: Its potential to evaluate beef meat conservation and aging.  
472 *Analytica Chimica Acta*, 901, 1-11. <https://doi.org/10.1016/j.aca.2015.08.032>
- 473 Chen, C., Guo, Z., Shi, X., Guo, Y., Ma, G., Ma, J., & Yu, Q. (2022). H<sub>2</sub>O<sub>2</sub>-induced oxidative stress  
474 improves meat tenderness by accelerating glycolysis via hypoxia-inducible factor-1 $\alpha$  signaling  
475 pathway in postmortem bovine muscle. *Food Chemistry: X*, 16, 100466.  
476 <https://doi.org/10.1016/j.fochx.2022.100466>
- 477 Chen, C., Zhang, J., Guo, Z., Shi, X., Zhang, Y., Zhang, L., Yu, Q., & Han, L. (2020). Effect of  
478 oxidative stress on AIF-mediated apoptosis and bovine muscle tenderness during postmortem  
479 aging. *Journal of Food Science*, 85(1), 77-85. <https://doi.org/10.1111/1750-3841.14969>
- 480 Della Malva, A., Gagaoua, M., Santillo, A., De Palo, P., Sevi, A., & Albenzio, M. (2022). First  
481 insights about the underlying mechanisms of Martina Franca donkey meat tenderization during  
482 aging: A proteomic approach. *Meat Science*, 193, 108925.  
483 <https://doi.org/10.1016/j.meatsci.2022.108925>
- 484 Hu, Z., Ma, Y., Liu, J., Fan, Y., Zheng, A., Gao, P., Wang, L., & Liu, D. (2022). Assessment of the  
485 Bioaccessibility of Carotenoids in Goji Berry (*Lycium barbarum* L.) in Three Forms: In Vitro  
486 Digestion Model and Metabolomics Approach. *Foods*, 11 (22), 3731.  
487 <https://doi.org/10.3390/foods11223731>
- 488 Huang, Y., Xie, Y., Li, Y., Zhao, M., Sun, N., Qi, H., & Dong, X. (2023). Quality assessment of  
489 variable collagen tissues of sea cucumber (*Stichopus japonicus*) body wall under different heat  
490 treatment durations by label-free proteomics analysis. *Food Research International*, 165,  
491 112540. <https://doi.org/10.1016/j.foodres.2023.112540>
- 492 Kagan, V. E., Mao, G., Qu, F., Angeli, J. P. F., Doll, S., Croix, C. S., Dar, H. H., Liu, B., Tyurin,  
493 V. A., Ritov, V. B., Kapralov, A. A., Amoscato, A. A., Jiang, J., Anthonymuthu, T.,  
494 Mohammadyani, D., Yang, Q., Proneth, B., Klein-Seetharaman, J., Watkins, S., Bahar, I.,  
495 Greenberger, J., Mallampalli, R. K., Stockwell, B. R., Tyurina, Y. Y., Conrad, M., & Bayır, H.  
496 (2017). Oxidized arachidonic and adrenic PEs navigate cells to ferroptosis. *Nature Chemical*  
497 *Biology*, 13(1), 81-90. <https://doi.org/10.1038/NCHEMBIO.2238>
- 498 Kim, Y. H. B., Ma, D., Setyabrata, D., Farouk, M. M., Lonergan, S. M., Huff-Lonergan, E., & Hunt,  
499 M. C. (2018). Understanding postmortem biochemical processes and post-harvest ageing  
500 factors to develop novel smart-ageing strategies. *Meat Science*, 144, 74-90.  
501 <https://doi.org/10.1016/j.meatsci.2018.04.031>
- 502 Lepper-Blilie, A. N., Berg, E. P., Buchanan, D. S., & Berg, P. T. (2016). Effects of post-mortem  
503 ageing time and type of ageing on palatability of low marbled beef loins. *Meat Science*, 112,  
504 63-68. <https://doi.org/10.1016/j.meatsci.2015.10.017>

- 505 Liang, C., Zhang, X., Yang, M., & Dong, X. (2019). Recent Progress in Ferroptosis Inducers for  
506 Cancer Therapy. *Advanced Materials*, 31(51), 1904197.  
507 <https://doi.org/10.1002/adma.201904197>
- 508 Liu, J., Hu, Z., Liu, D., Zheng, A., & Ma, Q. (2023). Glutathione metabolism-mediated ferroptosis  
509 reduces water-holding capacity in beef during cold storage. *Food Chemistry*, 398, 133903.  
510 <https://doi.org/10.1016/j.foodchem.2022.133903>
- 511 Liu, J., Hu, Z., Ma, Q., Wang, S., & Liu, D. (2023). Ferritin-dependent cellular autophagy pathway  
512 promotes ferroptosis in beef during cold storage. *Food Chemistry*, 412, 135550.  
513 <https://doi.org/10.1016/j.foodchem.2023.135550>
- 514 Liu, J., Hu, Z., Ma, Q., Yang, C., Zheng, A., & Liu, D. (2023). Reduced water-holding capacity of  
515 beef during refrigeration is associated within creased heme oxygenase 1 expression, oxidative  
516 stress and ferroptosis. *Meat Science*, 202, 109202.  
517 <https://doi.org/10.1016/j.meatsci.2023.109202>
- 518 Liu, J., Hu, Z., Zheng, A., Ma, Q., & Liu, D. (2022). Identification of exudate metabolites associated  
519 with quality in beef during refrigeration. *LWT - Food Science and Technology*, 172, 114241.  
520 <https://doi.org/10.1016/j.lwt.2022.114241>
- 521 Liu, J., Liu, D., Wu, X., Pan, C., Wang, S., & Ma, L. (2022). TMT quantitative proteomics analysis  
522 reveals the effects of transport stress on iron metabolism in the liver of chicken. *Animals*, 12(1),  
523 52. <https://doi.org/10.3390/ani12010052>
- 524 Liu, J., Liu, D., Zheng, A., & Ma, Q. (2022). Haem-mediated protein oxidation affects water-  
525 holding capacity of beef during refrigerated storage. *Food Chemistry: X*, 100304.  
526 <https://doi.org/10.1016/j.fochx.2022.100304>
- 527 Lombardi-Boccia, G., Martinez-Dominguez, B., & Aguzzi, A. (2002). Total heme and non-heme  
528 iron in raw and cooked meats. *Journal Of Food Science*, 67(5), 1738-1741.  
529 <https://doi.org/10.1111/j.1365-2621.2002.tb08715.x>
- 530 Marcondes Krauskopf, M., Darlan Leal de Araújo, C., dos Santos-Donado, P. R., Damiamas  
531 Baccarin Dargelio, M., Antônio Santos Manzi, J., Cecilia Venturini, A., César de Carvalho  
532 Balieiro, J., Francisquine Delgado, E., & Contreras-Castillo, C. J. (2023). The effect of  
533 succinate on color stability of Bos Indicus bull meat: pH-dependent effects during the 14-day  
534 aging period. *Food Research International*, 113688.  
535 <https://doi.org/10.1016/j.foodres.2023.113688>
- 536 Setyabrata, D., Ma, D., Xie, S., Thimmapuram, J., Cooper, B. R., Aryal, U. K., & Kim, Y. H. B.  
537 (2023). Proteomics and metabolomics profiling of meat exudate to determine the impact of  
538 postmortem ageing on oxidative stability of beef muscles. *Food Chemistry: X*, 18, 100660.  
539 <https://doi.org/10.1016/j.fochx.2023.100660>
- 540 Singhabahu, R., Kodagoda Gamage, S. M., & Gopalan, V. (2023). Pathological significance of  
541 heme oxygenase-1 as a potential tumor promoter in heme-induced colorectal carcinogenesis.



- 542 *Cancer Pathogenesis and Therapy*. <https://doi.org/10.1016/j.cpt.2023.04.001>
- 543 Wang, S., Wei, W., Ma, N., Qu, Y., & Liu, Q. (2022). Molecular mechanisms of ferroptosis and its  
544 role in prostate cancer therapy. *Critical Reviews in Oncology/Hematology*, 176, 103732.  
545 <https://doi.org/10.1016/j.critrevonc.2022.103732>
- 546 Wang, Y., Li, W., Zhang, C., Li, F., Yang, H., & Wang, Z. (2023). Metabolomic comparison of  
547 meat quality and metabolites of geese breast muscle at different ages. *Food Chemistry: X*, 19,  
548 100775. <https://doi.org/10.1016/j.fochx.2023.100775>
- 549 Wang, Z., Li, X., Lu, K., Wang, L., Ma, X., Song, K., & Zhang, C. (2023). Effects of dietary iron  
550 levels on growth performance, iron metabolism and antioxidant status in spotted seabass  
551 (*Lateolabrax maculatus*) reared at two temperatures. *Aquaculture*, 562, 738717.  
552 <https://doi.org/10.1016/j.aquaculture.2022.738717>
- 553 Weidinger, A., Milivojevic, N., Hosmann, A., Duvigneau, J. C., Szabo, C., Törö, G., Rauter, L.,  
554 Vaglio-Garro, A., Mkrtychyan, G. V., Trofimova, L., Sharipov, R. R., Surin, A. M.,  
555 Krasilnikova, I. A., Pinelis, V. G., Tretter, L., Moldzio, R., Bayır, H., Kagan, V. E., Bunik, V.  
556 I., & Kozlov, A. V. (2023). Oxoglutarate dehydrogenase complex controls glutamate-mediated  
557 neuronal death. *Redox Biology*, 62, 102669. <https://doi.org/10.1016/j.redox.2023.102669>
- 558 Xia, J., Si, H., Yao, W., Li, C., Yang, G., Tian, Y., & Hao, C. (2021). Research progress on the  
559 mechanism of ferroptosis and its clinical application. *Experimental Cell Research*, 409(2),  
560 112932. <https://doi.org/10.1016/j.yexcr.2021.112932>
- 561 Xia, X., Cheng, Z., He, B., Liu, H., Liu, M., Hu, J., Lei, L., Wang, L., & Bai, Y. (2021). Ferroptosis  
562 in aquaculture research. *Aquaculture*, 541, 736760.  
563 <https://doi.org/10.1016/j.aquaculture.2021.736760>
- 564 Xie, L., Fang, B., & Zhang, C. (2023). The role of ferroptosis in metabolic diseases. *Biochimica et*  
565 *Biophysica Acta (BBA) - Molecular Cell Research*, 1870(6), 119480.  
566 <https://doi.org/10.1016/j.bbamcr.2023.119480>
- 567 Yang, W. S., Kim, K. J., Gaschler, M. M., Patel, M., Shchepinov, M. S., & Stockwell, B. R. (2016).  
568 Peroxidation of polyunsaturated fatty acids by lipoxygenases drives ferroptosis. *Proceedings*  
569 *of the National Academy of Sciences*, 113(34), E4966-E4975.  
570 <https://doi.org/10.1073/pnas.1603244113>
- 571 Yu, Q., Cooper, B., Sobreira, T., & Kim, Y. H. B. (2021). Utilizing Pork Exudate Metabolomics to  
572 Reveal the Impact of Ageing on Meat Quality. *Foods*, 10(3), 668.  
573 <https://doi.org/10.3390/foods10030668>
- 574 Yu, Q., Li, S., Cheng, B., Brad Kim, Y. H., & Sun, C. (2023). Investigation of changes in proteomes  
575 of beef exudate and meat quality attributes during wet-aging. *Food Chemistry: X*, 17, 100608.  
576 <https://doi.org/10.1016/j.fochx.2023.100608>
- 577 Zhang, J., Yu, Q., Han, L., Han, M., & Han, G. (2020). Effects of lysosomal iron involvement in

578 the mechanism of mitochondrial apoptosis on postmortem muscle protein degradation. *Food*  
579 *Chemistry*, 328, 127174. <https://doi.org/10.1016/j.foodchem.2020.127174>

580 Zhang, N., Yu, X., Song, L., Xiao, Z., Xie, J., & Xu, H. (2022). Ferritin confers protection against  
581 iron-mediated neurotoxicity and ferroptosis through iron chelating mechanisms in MPP+  
582 induced MES23.5 dopaminergic cells. *Free Radical Biology and Medicine*, 193, 751-763.  
583 <https://doi.org/10.1016/j.freeradbiomed.2022.11.018>

584 Zhang, Y., Tian, X., Jiao, Y., Wang, Y., Dong, J., Yang, N., Yang, Q., Qu, W., & Wang, W. (2022).  
585 Free iron rather than heme iron mainly induces oxidation of lipids and proteins in meat cooking.  
586 *Food Chemistry*, 382, 132345. <https://doi.org/10.1016/j.foodchem.2022.132345>

587

### 588 **Credit Author Statement**

589 Conceptualization, Jun Liu and Dunhua Liu; Data curation, Jun Liu; For-mal analysis,  
590 Jun Liu Hui Yue, and He Li; Funding acquisition, Cuili Pan and Dunhua Liu;  
591 Investigation, Jun Liu, Yuanliang Hu, Xiang Yu, Weiwei Dong, and Yanli Feng;  
592 Methodology, Jun Liu; Project administration, Dunhua Liu; Re-sources, Jun Liu;  
593 Supervision, Cuili Pan and Dunhua Liu; Validation, Jun Liu; Visualization, Jun Liu and  
594 Dunhua Liu; Writing - original draft, Jun Liu; Writing - review & editing, Jun Liu and  
595 Ziyang Hu.

596

597

### 598 **Figure legends**

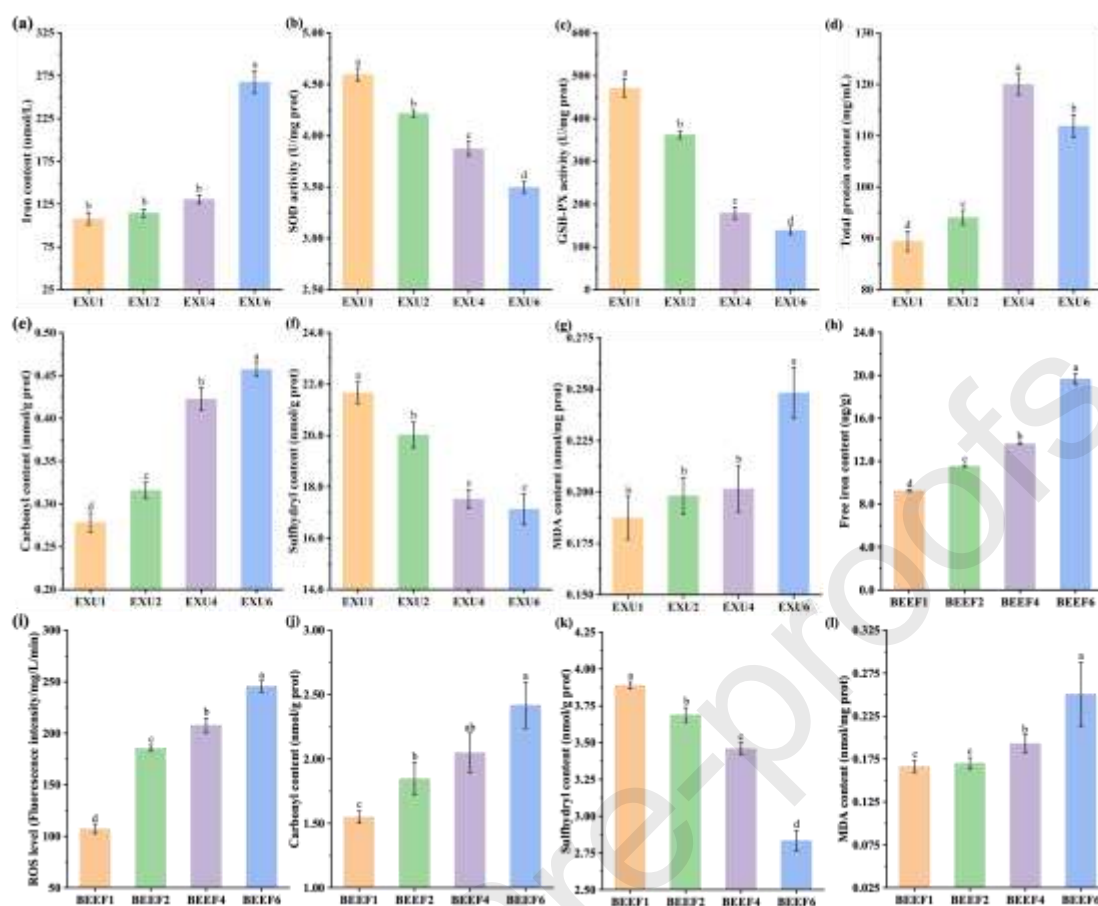
599 (If the PDF file is not clear, please download the Word file for review)

600

601

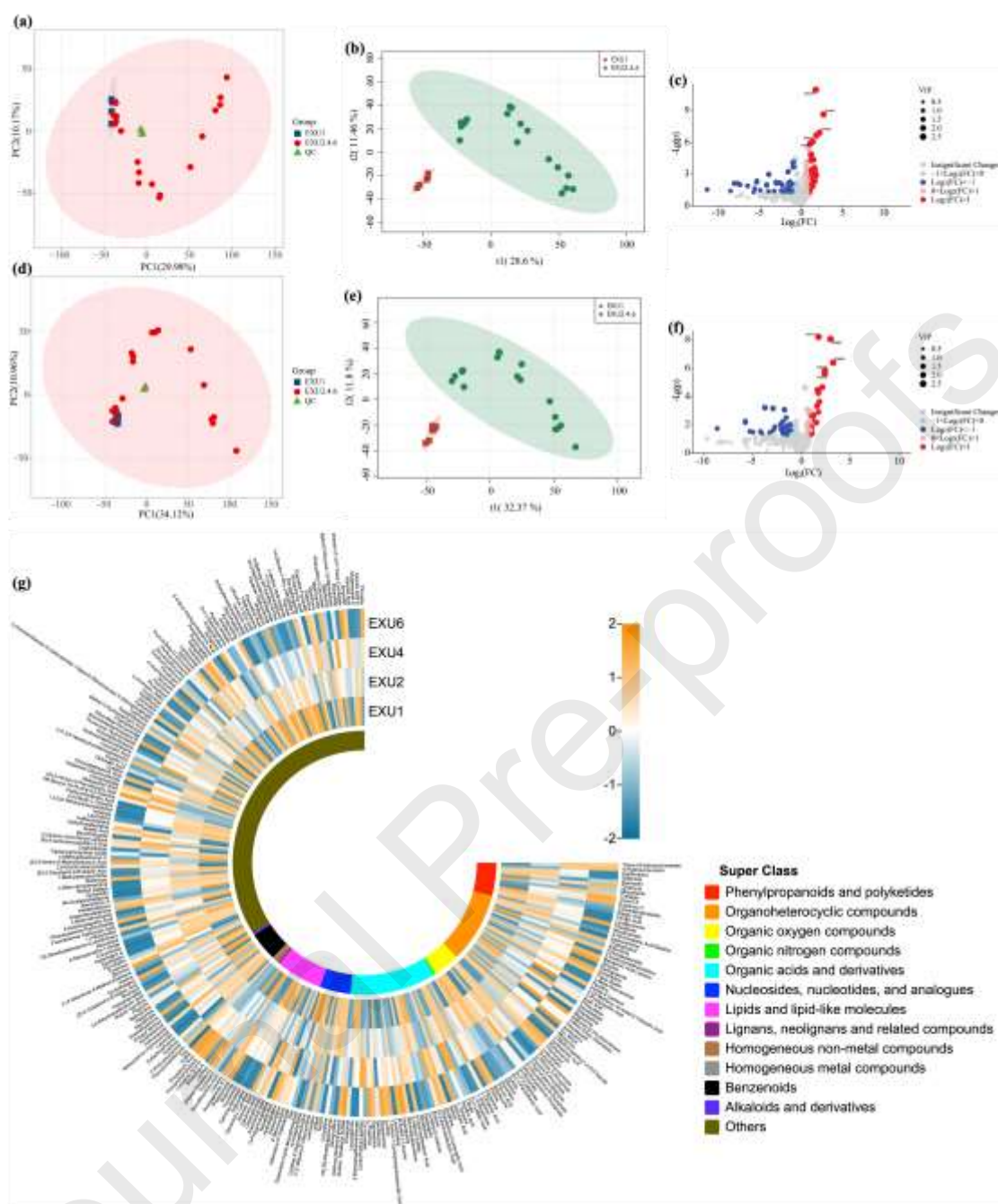
602

603



604

605 **Fig. 1** Exudate and beef iron ion levels and oxidation status. (a) Iron content in exudate. (b) SOD  
 606 activity in exudate. (c) GSH-PX activity in exudate. (d) Total protein content in exudate. (e)  
 607 Protein carbonyl level in exudate. (f) Protein sulfhydryl level in exudate. (g) MDA level in  
 608 exudate. (h) Free iron content in beef tissues. (i) ROS levels in beef tissues. (j) Protein carbonyl  
 609 levels in beef tissue. (k) Protein sulfhydryl level in beef tissue. (l) Beef tissue MDA levels. a-e  
 610 different lowercase letters indicate one-way *t*-test  $P < 0.05$ .



611

612 **Fig. 2** Metabolite profiles based on metabolomics. (a) PCA analysis of metabolites in POS. (b)

613 PLS-DA analysis of metabolites in POS. (c) Volcano map for screening DMs in POS. (d) PCA

614 analysis of metabolites in NEG. (e) PLS-DA analysis of metabolites in NEG. (f) Volcano map for

615 screening DMs in NEG. (g) Heat map of clustering of DMs.

616

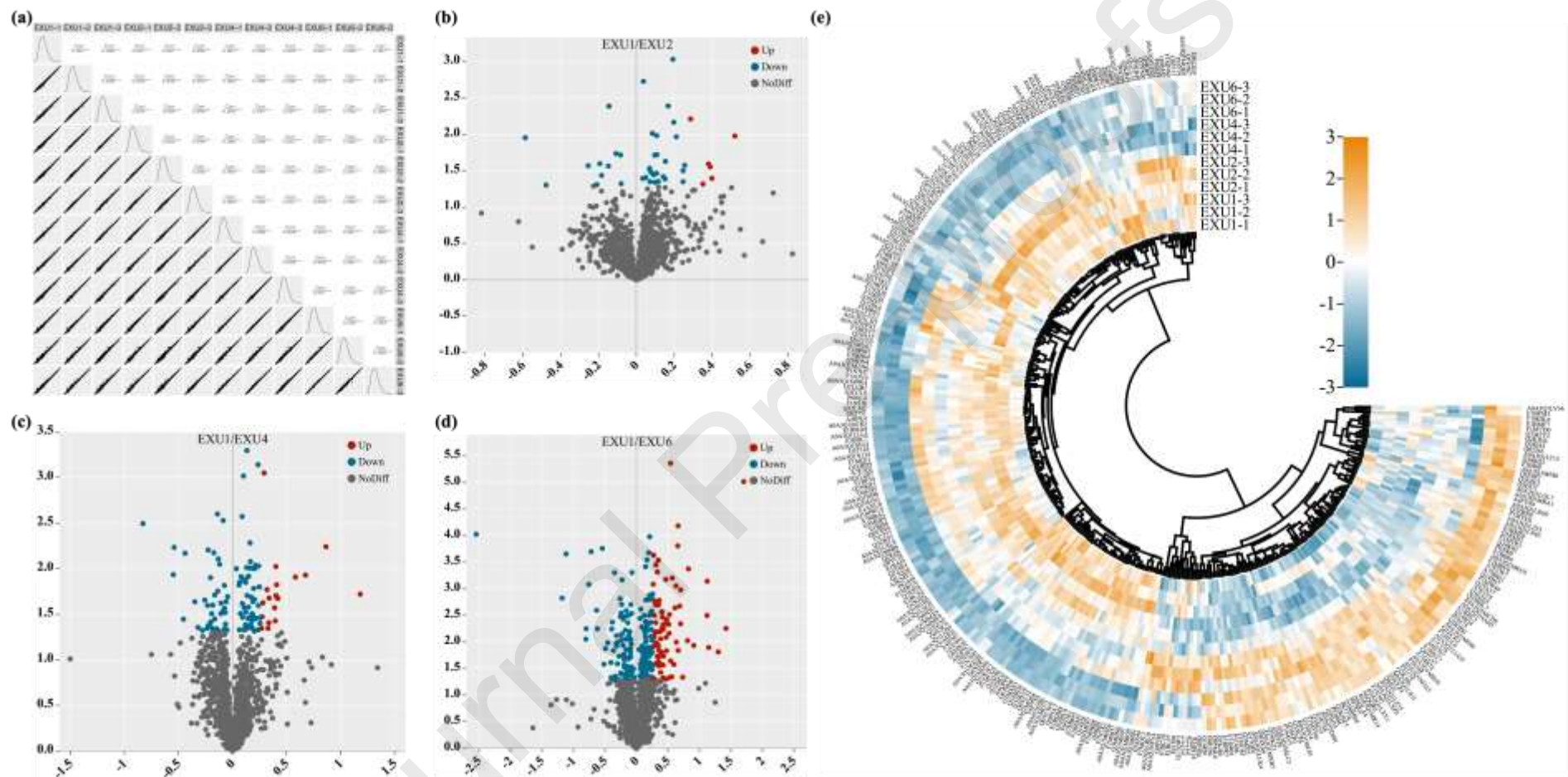


**Fig. 3** Protein profiles based on proteomics. (a) Correlation coefficient plots of protein expression patterns of different groups. (b) Volcano map of DEPs between B1 and B2. (c) Volcano map of DEPs between B1 and B4. (d) Volcano plot of DEPs between B1 and B6. (e) Heat map of clustering of DEPs.

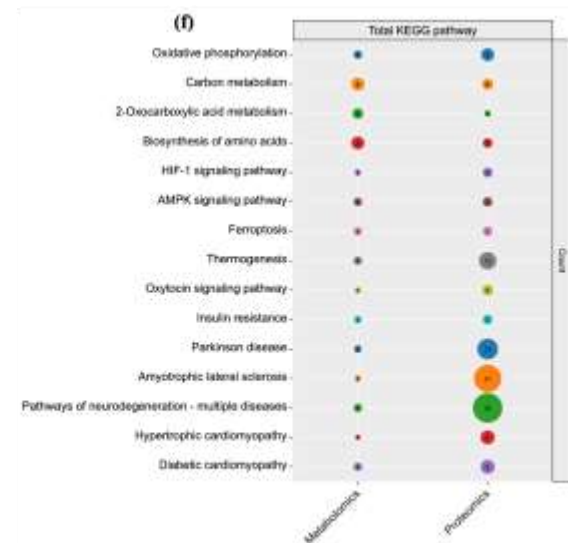
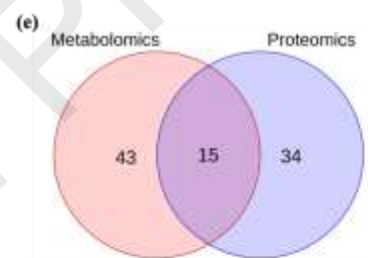
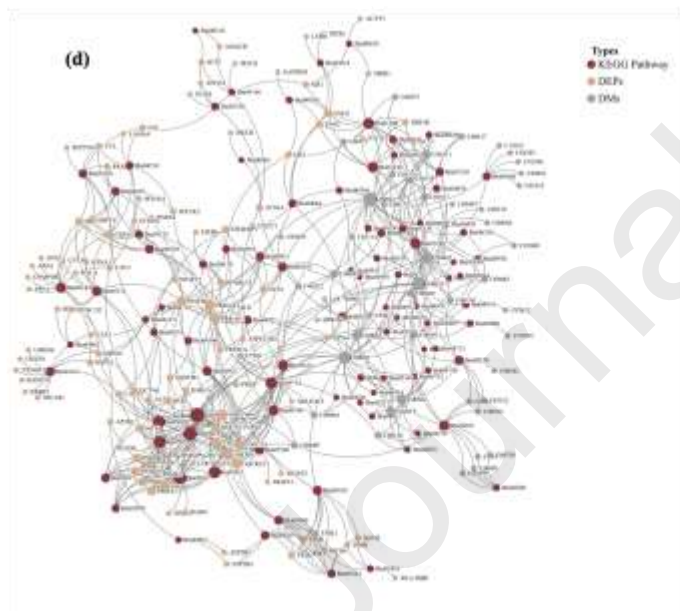
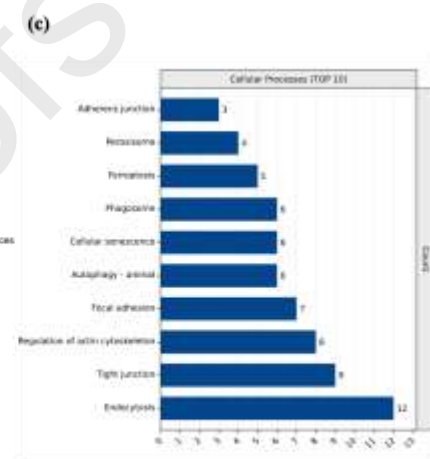
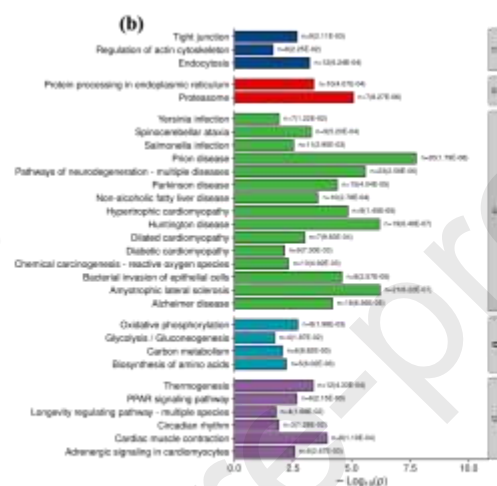
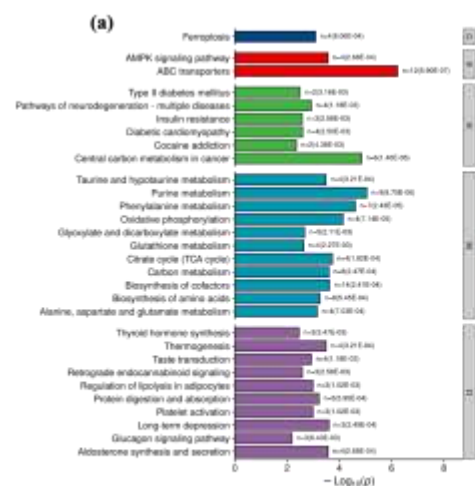
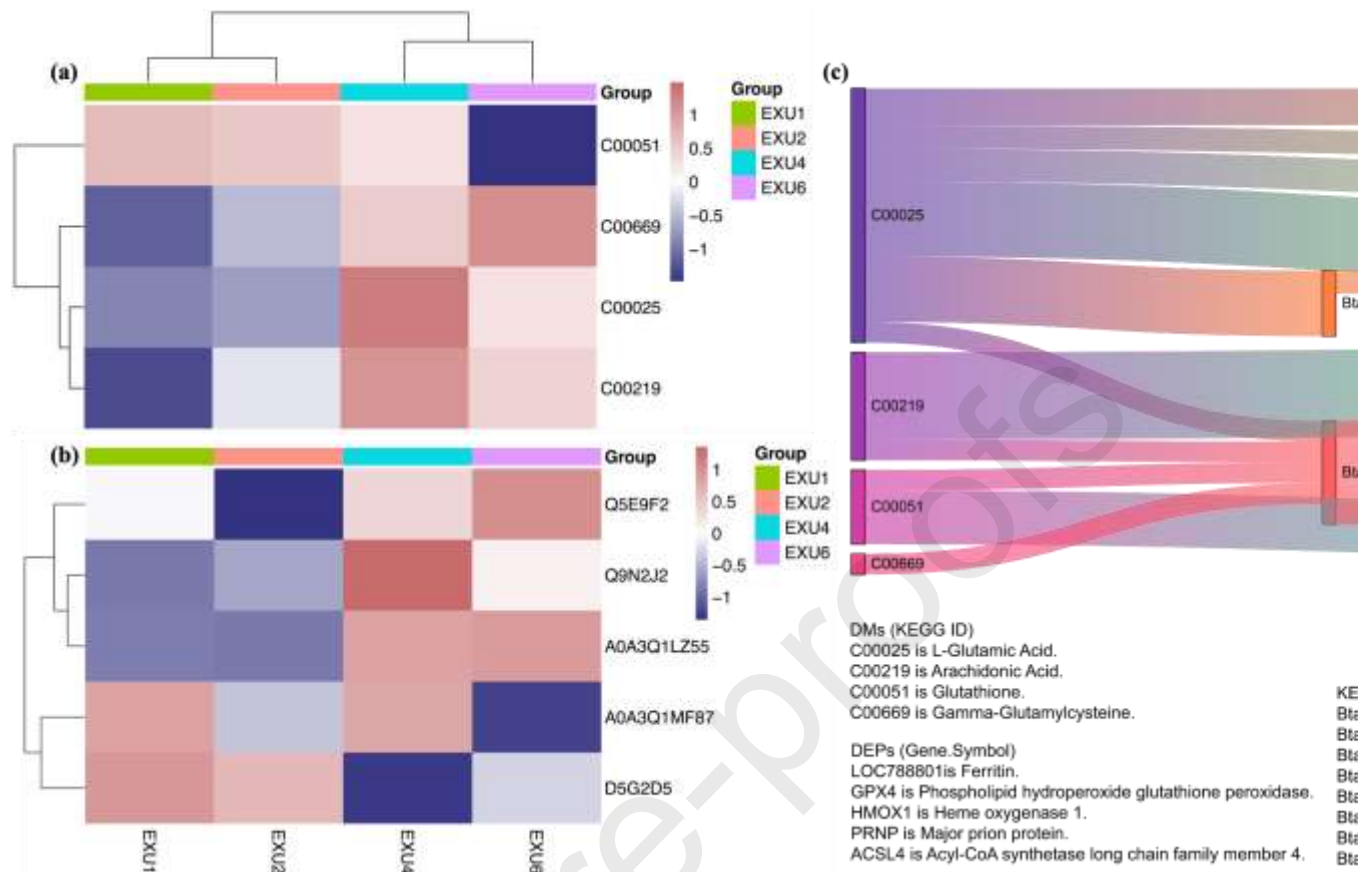


**Fig. 4** Metabolic pathway analysis based on metabolomics and proteomics. (a) KEGG enrichment pathway analysis based on metabolomics. (b) KEGG enrichment pathway analysis based on proteomics. (c) Proteomics-based cellular process pathways for KEGG enrichment (top 10). (d) Network diagram of metabolomics and proteomics combined analysis. (e) Venn diagram of KEGG enrichment pathways based on metabolomics and proteomics. (f) Shared pathways of metabolomics and proteomics based on KEGG enrichment. C is Cellular Processes, E is Environmental Information Processing, H is Human Diseases, M is Metabolism, O is Organismal Systems.

Journal Pre-proof



1

2 **Fig. 5** Iron metabolism pathway. (a) Cluster heat map of DMs involved in iron metabolism. (b)

3 Heat map of DEPs involved in iron metabolism. (c) Sankey diagram of the interaction network of

4 DMs-DEPs-metabolic pathways based on ferroptosis pathways. A0A3Q1MF87 is ferritin,

5 Q9N2J2 is phospholipid hydroperoxide glutathione peroxidase, Q5E9F2 is heme oxygenase 1,

6 D5G2D5 is major prion protein, A0A3Q1LZ55 is acyl-CoA synthetase long chain family member

7 4.

8

9 **Highlights**

10

11 1) Metabolomics and proteomics analysis of exudate were used to characterize the  
12 effect of iron metabolism on beef oxidation.

13 2) Ferroptosis was the major iron metabolic pathway during beef ageing.

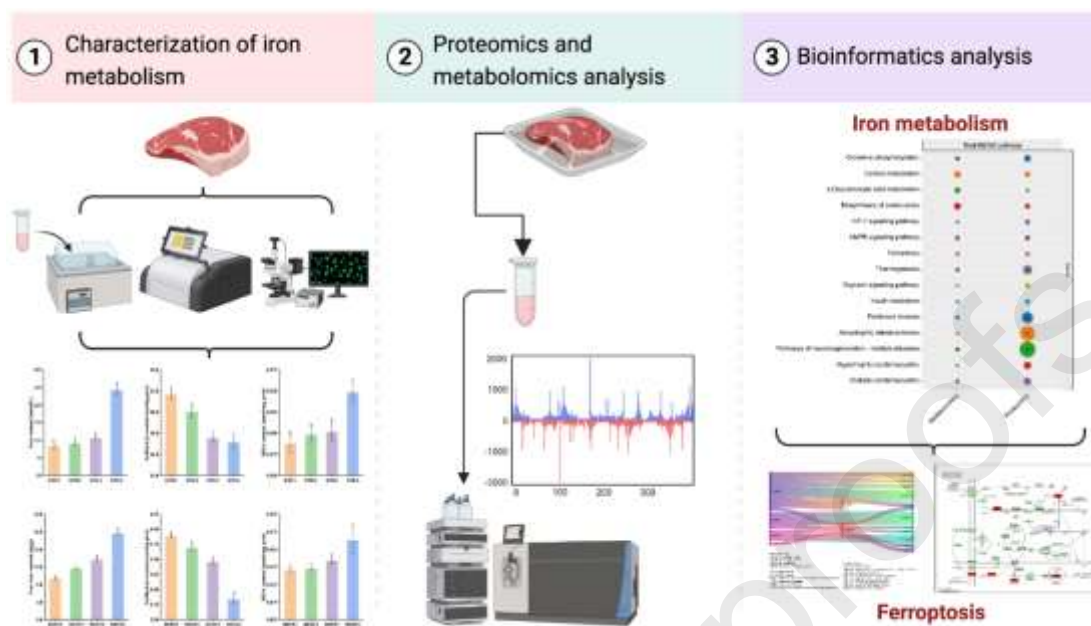
14 3) Disturbed iron metabolism was dependent on free iron accumulation.

15 4) Free iron induced oxidative stress in muscle tissue through the Fenton reaction.

16



17



18